Accepted Manuscript

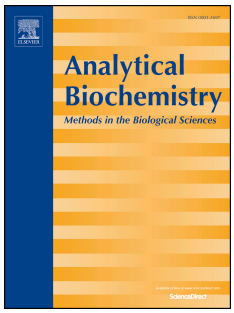

Characterization of binding and quantification of human autoantibodies to PDGFRα using a biosensor-based approach

Gianluca Moroncini, Massimiliano Cuccioloni, Ph.D., Matteo Mozzicafreddo, Katarzyna Natalia Pozniak, Antonella Grieco, Chiara Paolini, Cecilia Tonnini, Tatiana Spadoni, Silvia Svegliati, Ada Funaro, Mauro Angeletti, Armando Gabrielli

PII: S0003-2697(17)30179-3

DOI: 10.1016/j.ab.2017.04.011

Reference: YABIO 12678

To appear in: *Analytical Biochemistry*

Received Date: 15 December 2016

Revised Date: 18 April 2017

Accepted Date: 20 April 2017

Please cite this article as: G. Moroncini, M. Cuccioloni, M. Mozzicafreddo, K.N. Pozniak, A. Grieco, C. Paolini, C. Tonnini, T. Spadoni, S. Svegliati, A. Funaro, M. Angeletti, A. Gabrielli, Characterization of binding and quantification of human autoantibodies to PDGFRα using a biosensor-based approach, *Analytical Biochemistry* (2017), doi: 10.1016/j.ab.2017.04.011.

TITLE

Characterization of binding and quantification of human autoantibodies to PDGFRα using a biosensor-based approach

AUTHORS

Gianluca Moroncini[1,2,¶], Massimiliano Cuccioloni[3,¶,*], Matteo Mozzicafreddo[3], Katarzyna Natalia Pozniak[1,4], Antonella Grieco[1], Chiara Paolini[1], Cecilia Tonnini[1], Tatiana Spadoni[1], Silvia Svegliati[1], Ada Funaro[5], Mauro Angeletti[3] and Armando Gabrielli[1,2].

[¶] These authors equally contributed to the work

ADDRESSES

[1] Dipartimento di Scienze Cliniche e Molecolari, Università Politecnica delle Marche - Ancona, Italy.

[2] Clinica Medica, Ospedali Riuniti Ancona, Italy.

[3] School of Biosciences and Veterinary Medicine, University of Camerino - Camerino, Italy

[4] Queensland Institute of Medical Research and School of Medicine, University of Queensland, Brisbane QLD, Australia

[5] Dipartimento di Scienze Mediche, Università di Torino, Italy

[*] **CORRESPONDING AUTHOR**

Massimiliano Cuccioloni, Ph.D.

School of Biosciences and Veterinary Medicine, University of Camerino

Via Gentile III da Varano – 62032 Camerino, Italy

Tel: +39 0737 403247

E-mail: massimiliano.cuccioloni@unicam.it

KEYWORDS

Biosensor; Systemic Sclerosis; PDGFR; Binding kinetics; Autoantibody quantification.

SUBJECT CATEGORY

Immunological procedures

ABSTRACT

Systemic sclerosis (SSc) is a chronic autoimmune disease of the connective tissue. The variety and clinical relevance of autoantibodies in SSc patients have been extensively studied, eventually identifying agonistic autoantibodies targeting the platelet-derived growth factor receptor alpha (PDGFRα), and representing potential biomarkers for SSc.

We used a resonant mirror biosensor to characterize the binding between surface-blocked PDGFRα and PDGFRα-specific recombinant human monoclonal autoantibodies (mAbs) produced by SSc B cells, and detect/quantify serum autoimmune IgG with binding characteristics similar to the mAbs. Kinetic data showed a conformation-specific, high-affinity interaction between PDGFRα and mAbs, with equilibrium dissociation constants in the low-to-high nanomolar range. When applied to total serum IgG, the assay discriminated between SSc patients and healthy controls, and allowed the rapid quantification of autoimmune IgG in the sera of SSc patients, with anti-PDGFRα IgG falling in the range 3.20-4.67 neq/L of SSc autoantibodies. The test was validated by comparison to direct and competitive anti-PDGFRα antibody ELISA. This biosensor assay showed higher sensibility with respect to ELISA, and other major advantages such as the specificity, rapidity, and reusability of the capturing surface, thus representing a feasible approach for the detection and quantification of high affinity, likely agonistic, SSc-specific anti-PDGFRα autoantibodies.

1. INTRODUCTION

The term Systemic sclerosis, or scleroderma, designates a heterogeneous autoimmune connective tissue disease characterized by distinct clinical patterns, which often display dramatically different clinical outcomes as different as a long survival time with limited morbidity and a decreased lifespan with huge disability [1]. One of the main limitations in the clinical management of SSc patients, once diagnosis has been formulated, is the lack of biomarkers predicting disease evolution and correlating with disease activity and severity. In fact, currently available biomarkers are certainly useful for SSc diagnosis, sub-classification and association with organ involvement [2], but none of them is sensitive to disease changes. To fill this gap, our group has focused the attention on serum anti-PDGFRα autoantibodies characterized by possessing stimulatory activity, both *in vitro* on human cells involved in SSc pathogenesis [3, 4] and *in vivo* on regenerated human skin engrafted onto mice [5], under the hypothesis that biologically active autoantibodies may correlate better with disease activity. One major problem with the validation of this hypothesis was the inability of detecting serum anti-PDGFRα antibodies with standard methods [6-8]. Recently, this problem has been partly solved by identifying the PDGFRα epitopes bound by these autoantibodies. We discovered that distinct PDGFRα epitopes are recognized by agonistic and non-agonistic autoantibodies, and used the peptides corresponding to these epitopes to detect the presence of agonistic autoantibodies in the serum of SSc patients but not in healthy controls [9]. However, this method, a competitive ELISA based on molar excess of soluble peptides added to serum samples before PDGFRα binding detection, does not permit quantification of SSc antibodies, limiting their potential as biomarkers usable to dissect the different clinical phases of this chronic disease. To address this issue, we adapted our previously described PDGFRα biosensor [10] to measure and compare the reactivity of agonistic and non-agonistic human anti-PDGFRα autoantibodies cloned from SSc B cells, and applied the binding kinetics of the monoclonal antibody possessing higher

agonistic activity towards the PDGFRα to calibrate the biosensor, eventually developing a quantitative biosensor-based assay. We describe herein this analytical method able to rapidly and reliably detect and quantify anti-PDGFRα serum IgG autoantibodies with nanomolar sensitivity.

2. MATERIALS AND METHODS

2.1. Materials and devices

$CuSO_4$, HCl, NaOH, NaCl, KCl, NaH_2PO_4 were obtained from Mallinckrodt Baker (Milan, Italy). Tween-20, G 418 disulphate salt and SDS were from Sigma-Aldrich (Milan, Italy). Carboxylate-functionalized cuvettes and the immobilization chemicals (N-hydroxysuccinimide (NHS), 1-ethyl-3-(3-dimethylaminopropyl)-carbodiimide (EDC), and ethanolamine) were obtained from Neosensors (Crewe, UK). All chemicals were of highest purity available.

Human PDGF-BB and mouse anti-human PDGFRα monoclonal antibody mab322 were obtained from R&D Systems (Milan, Italy). Fluorescein isothiocyanate labelled secondary antibody was obtained from Jackson Immunoresearch (PA, USA). Rabbit anti-human PDGFRα antibody D01P was obtained from Abnova (Taipei, Taiwan). HRP-conjugated goat anti-rabbit IgG was obtained from Santa Cruz (Heidelber, Germany).

pcDNA V5 HIS A vector and Lipofectamine 2000 were obtained from Invitrogen (Milan, Italy) HeLa cells were obtained from ATCC (Rockville, TX, USA).

Human PDGFRα and recombinant human monoclonal autoantibodies (mAb), namely V_HPAM-V_κ13B8, V_HPAM-V_κ16F4, V_HPAM-V_λ16F4, and V_HPAM-V_λ13B8) were produced and purified as previously reported [9, 11].

Binding analyses were carried out on an evanescent wave/resonant mirror [12] optical biosensor (IAsys plus - Affinity Sensors Ltd, Cambridge, UK). The resonant mirror apparatus (consisting of a high-refractive-index dielectric coupling layer deposited on a silica glass prism waveguide [13], with a low-refractive-index hafnium oxide layer interposed) is integrated in an open two-wells cuvette structure, with the sensing surface being exposed to the solution contained within the

cuvette lumen. Soluble ligands, reagents and buffers can be added by manual pipetting, and removed using an integrated vacuum aspiration system. A micro-stirrer is included to ensure rapid sample mixing and to prevent limits due to diffusion.

Chromatographic analyses were performed on an AKTA Basic System (GE Healthcare, Milan, Italy), using HiTrap metal-chelating columns obtained from GE Healthcare (Milan, Italy), and a Tosoh Progel^{TM}-TSK G2000 SWXL column, 30 cm × 7.8 mm (Sigma Aldrich, Milan, Italy).

2.2. Immobilization of rhPDGFRα-His

rhPDGFRα-functionalized surfaces were obtained as previously reported [10]. Briefly, carboxylate cuvettes were rinsed with PBS pH 7.4, and activated with an equimolar solution of EDC and NHS [14]. rhPDGFRα-His was solubilized in 10 mM CH_3COONa buffer pH 4.5, then anchored to the carboxylic surface via the N-terminus of histidine tail. To achieve optimal surface density, we tested different rhPDGFRα concentrations in the range 100-800 μg/mL: the concentration 300 μg/mL was finally selected as it provided an adequate number of binding sites, and at the same time prevented the dimerization between blocked rhPDGFRα macromolecules that could reduce the number of available binding sites on the sensing surface [9]. In detail, 100, 200 and 800 μg/mL rhPDGFRα solutions yielded to surfaces with lower sensibility (rhPDGFRα surface resulting from 100 and 200 μg/mL solutions was characterized by lower surface density/number of binding sites for SSc autoantibodies; rhPDGFRα surface resulting from 800 μg/mL solution, irrespective of higher surface density, was characterized by a lower number of effectively available binding for SSc autoantibodies, both because of steric hindrance and rhPDGFRα dimerization). Next, free carboxylic sites on the sensor surface were blocked by injection of 1 M ethanolamine, pH 8.5. The surface was finally re-equilibrated with PBS (pH=7.4). Following immobilization, negative baseline drift signals were not observed with time or multiple PBS (pH=7.4) washes, confirming that the

receptor molecules were irreversibly linked to the sensor surface. The resulting shift in sensor response indicated the coupling of a partial 'Langmuir' layer (70% surface occupancy) corresponding to a final surface density of 1.7 ng/mm^2, approximately equivalent to 7 mg/mL (see Supplementary Material for details). The use of CH_3COONa 10 mM, pH 4.5 as immobilization buffer (chosen upon the PDGFRα isoelectric point=5.5) allowed an efficient immobilization, while preserving the native-like conformation of the receptor, as assessed by PDGF-BB and anti-PDGFRα mab322, which can recognize only conformational binding sites of the extracellular PDGFRα domain. Specifically, prior to each experimental session, association kinetics were monitored upon independent additions of PDGF-BB and mab322 (2.50 nM each) to surface-blocked rhPDGFRα for about 1 min (the time interval required to reach the equilibrium between association and dissociation events). Dissociation steps were performed with a single PBS buffer wash (pH=7.4), whereas the baseline corresponding to non-complexed rhPDGFRα was recovered by serial PBS (pH 5.5) washes (approximately 10 min). Conformational controls were randomly repeated during analyses of IgG samples. Local and global fit analysis of the interaction data generally revealed monophasic kinetics. Specifically, mono-exponential analysis of association curves residuals was not affected by measurable systematic errors (a bi-exponential model did not significantly improve the quality of the fit as judged by an F-test, 95% confidence). The biosensor chamber was thermostatted at 25°C throughout.

2.3. Derivation of binding kinetics of PDGF-BB to rhPDGFRα-functionalized surface

Kinetic parameters of the interaction between PDGF-BB and rhPDGFRα were determined by individual additions of 0.13, 0.26, 1.33 and 2.66 nM PDGF-BB (three replicates each). Association kinetics were followed for about 1 min (the time interval requested to reach the maximal response at equilibrium for the highest concentration of PDGF-BB tested). The dissociation of each complex was achieved with a single PBS (pH=7.4) wash (dissociation phases were followed for 1 min),

whereas baseline recovery (regeneration of non-complexed rhPDGFRα surface) was obtained with multiple PBS (pH 5.5). Regeneration procedure times ranged between 5 and 15 min, depending upon PDGF-BB concentration.

2.4. Binding of recombinant human mAbs to rhPDGFRα-functionalized surface

Recombinant human mAbs were independently added at different concentrations in the range 0.58-16 nM onto the rhPDGFRα-coated surface, and association kinetics were routinely followed up to equilibrium. Dissociation steps and surface regeneration were performed by addition of fresh buffer (PBS pH=7.4 and pH=5.5, respectively), each time assessing the baseline recovery prior to any further addition of soluble recombinant human mAbs. Raw data were globally fitted to a classic monophasic model:

$$R_t = R_{eq,[\text{recombinant human mAb}]}\left(1 - e^{-(k_{ass}[\text{recombinant human mAb}]+k_{diss})t}\right) \quad \text{(Eq.1)}$$

where R_t is the response at time *t*,

$$R_{eq,[\text{recombinant human mAb}]} = \frac{R_{max}[\text{recombinant human mAb}]k_{ass}}{k_{diss}+[\text{recombinant human mAb}]k_{ass}} \quad \text{(Eq.2)}$$

R_{max} is the maximal response at asymptotically high concentrations of [recombinant human mAb], and k_{ass} and k_{diss} are the kinetic association and dissociation constants, respectively. Data analysis and fitting was performed with FAST Fit software.

2.5. Serum samples

Serum samples obtained from 8 patients with a definite diagnosis of SSc [15] and 8 healthy controls (HC) were selected upon previous results obtained by anti-PDGFRα antibody competitive ELISA

[9], choosing as many positive samples as possible, and with the most homogeneous frequency distributions of OD values. The clinical features of SSc patients included in this study are summarized in Table 1. All participants gave informed consent for use of blood samples in this study. Ethics committee approval document is provided as Supplemental Material.

Number of patients	**8**
Sex; female/male ratio	3/1
Age; median age (age range) (years)	48 [25-68]
Limited/diffuse	3/1
Duration of disease: average duration of disease (years)	9
Rodnan Skin Score: average Rodnan Skin Score	10
ANA (% positive)	75%
Anti-Scl 70 (% positive)	50%
Anticentromere antibody (% positive)	37.5%
Internal organ involvement; % of lung and/or GI tract and/or heart involvement	75.0%

Table 1. Clinical characteristics of SSc patients.

2.6. Purification of IgG from serum

IgG were purified from the SSc and HC sera, selected as indicated above, using individual A/G resin columns (Pierce) as previously described [10]. After elution with glycine at pH 2.2 and neutralization with Tris buffer, the fractions containing IgG were subjected to size exclusion chromatography (5000 MWCO, Thermo Scientific) to remove trace amounts of contaminating cytokines. The absence of PDGF in IgG preparations was checked by immunoblotting with a

primary polyclonal rabbit anti-human PDGF-BB antibody (Abcam) with detection limit of 0.1 ng cytokine/200 μg IgG. IgG samples were identified with a numerical code.

2.7. Binding of serum IgG to rhPDGFRα-functionalized biosensor

IgG samples were individually added to the PDGFRα-functionalized surface, and each response kinetic was monitored up to equilibrium. The dissociation of the complexes and the regeneration of the PDGFRα monolayer were carried out by serial PBS washes. Each IgG sample was analysed in triplicate. Values falling outside the 95% confidence interval were considered significantly different from controls. Detection procedures were replicated on different days (n=3) both on the same and on different rhPDGFRα-functionalized surfaces (n=3) to assess the inter-day and the "surface-to-surface" variability. Analyses of SSc IgG samples were always performed in triplicate. Additionally, the number of regeneration cycles that the sensor surface could withstand without significant loss of assay sensitivity and accuracy, and the stability of the sensing surface throughout multiple measurements were evaluated and assessed.

2.8. Immunoenzymatic assays (ELISAs)

All IgG samples were tested by direct and competitive anti-PDGFRα antibody ELISA as previously described [9]. A standard hyperbolic calibration curve was used to estimate the concentration of anti-PDGFRα antibody from absorbance units.

2.9. Limits of Detection and Quantitation

In compliance with the IUPAC rules [16], the limits of detection (LOD) and quantification (LOQ) of both ELISA and biosensor assays were calculated as three and ten times the standard deviation of the blank measurements, respectively. IgG purified from HC sera were used as a blank reference.

2.10. Statistical Analysis

Results were expressed as mean values ± standard deviation of results obtained from at least three separate experiments. Statistical analysis was performed with one-way ANOVA, followed by the Bonferroni test using Sigma-stat 3.1 software (SPSS, Chicago, IL, USA). *p* values <0.05 and <0.01 were considered statistically significant.

3. RESULTS

3.1. Binding kinetics and binding specificity of recombinant human mAbs

First, we characterized the binding of recombinant human mAbs [9] to surface-blocked rhPDGFRα, whose native-like folding was assessed by conformational ligands, as described in the Material and Methods section (Fig.1, Panel A).

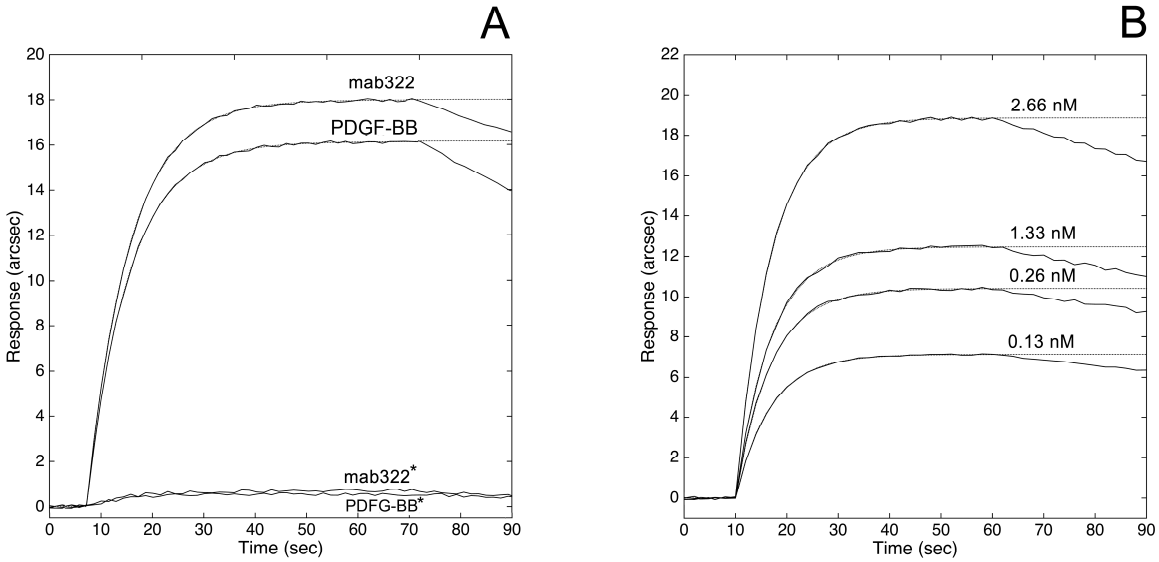

Fig.1. **Conformational control check (Panel A)**. Overlay of association and dissociation kinetics of mab322 and PDGF-BB (solid lines) to a surface-blocked native-like rhPDGFRα and to a partially denatured counterpart (emphasized by asterisks). The fit to a standard mono-exponential model is plotted as dotted lines. **Binding of soluble PDGF-BB to immobilized rhPDGFRα (Panel B)**. Overlay of association and dissociation kinetics measured at increasing concentrations of PDGF-BB (solid lines), and the fit thereof to a standard mono-exponential model (dotted lines).

PDGF-BB bound PDGFRα with the highest affinity (K_D = 0.23 ± 0.02 nM) (Fig.1, Panel B) compared to V_HPAM-V_κ13B8, V_HPAM-V_κ16F4 and V_HPAM-V_λ16F4 recombinant human mAbs (K_D = 184 ± 19 nM, 71 ± 13 nM and 17 ± 5 nM, respectively), whereas V_HPAM-V_λ13B8 recombinant human mAb did not bind to PDGFRα (Fig.2).

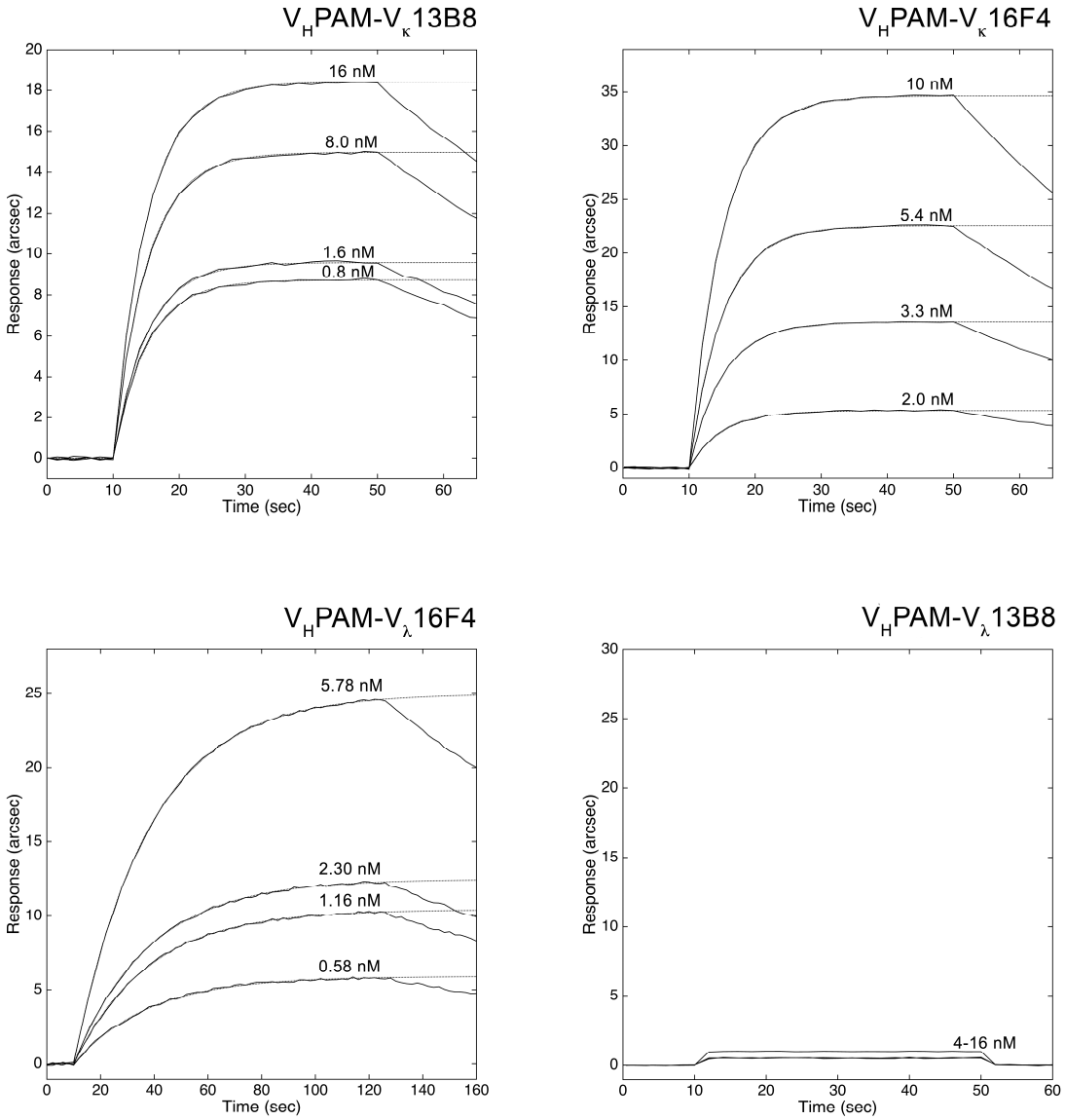

Fig.2. Binding of soluble rHumaab to immobilized rhPDGFR*α*. Overlay of association and dissociation kinetics measured at increasing concentrations of V_HPAM-V_κ13B8, V_HPAM-V_κ16F4, V_HPAM-V_λ16F4 (solid lines), and the fit thereof to a standard mono-exponential model (dotted lines). Response upon addition of non-binding V_HPAM-V_λ13B8 is reported as a control of specificity.

The analysis of the association/dissociation rate constants further dissected the binding properties of the different ligands to PDGFRα. Specifically, the different affinities to rhPDGFRα of PDGF-BB and recombinant human mAbs were dependent on the 10-fold faster recognition process (k_{ass}= (3 ±

0.2)×10^7 $M^{-1}s^{-1}$) of PDGF-PDGFRα complexes compared to recombinant human mAb-PDGFRα complexes (all characterized by k_{ass} values ranging between (1.8 ± 0.6)×10^6 and (2.8 ± 0.4)×10^6 $M^{-1}s^{-1}$). Conversely, differences in equilibrium constants among recombinant human mAbs were dependent on dissociation rate constants (k_{diss} = 0.035 ± 0.002 s^{-1}, 0.02 ± 0.003 s^{-1}, and 0.003 ± 0.001 s^{-1}, for V_HPAM-V_κ13B8, V_HPAM-V_κ16F4 and V_HPAM-V_λ16F4, respectively). To further assess the binding specificity of the recombinant human mAbs, the assay was repeated with immobilized human PDGFRβ-His. The recombinant human mAbs, either used at the same concentration or six-fold higher, did not bind to natively folded PDGFRβ (data not shown).

3.3. Calibration Curve

Based on the high affinity for rhPDGFRα and the better confidence limits for dose-response curve compared with the other anti-PDGFRα recombinant human mAbs (as assessed by Student's t-test applied at 95% confidence level), V_HPAM-V_κ16F4 was chosen to generate a calibration curve. Thus, V_HPAM-V_κ16F4 was added to the surface-immobilized PDGFRα-His at different concentrations in the range 1-10 nM (Fig.3), and association kinetics were monitored up to equilibrium (R_{eq}). The plot of R_{eq} versus V_HPAM-V_κ16F4 concentration showed the hyperbolic correlation:

$$R_{eq} = \frac{R_{max}[V_H PAM\text{-}V_k 16F4]}{K_{D,ext} + [V_H PAM\text{-}V_k 16F4]} \qquad \text{(Eq.3)}$$

where R_{max} is the response at asymptotically high concentrations of the autoantibody. This calibration procedure was replicated on three different days. Under the experimental conditions described above, the determination of IgG at sub-saturating concentrations ([IgG] < K_D) assured a good reproducibility of the assay on different rhPDGFRα-functionalized surfaces. Moreover, the reversibility of the interaction enabled the achievement of an unambiguous response upon IgG

binding within 2 minutes. Fit (solid line) and 95% confidence bound (dashed lines) are reported in Fig.3, R^2 being equal to 0.9989. Best fitted values for R_{max} and $K_{D,ext}$ were 153±20 arcsec and 35±16 nM (the value of the $K_{D,ext}$ being in strong agreement with the value calculated from kinetic data). Calibration data were expressed throughout as equivalents of V_HPAM-V_κ16F4 *per* litre.

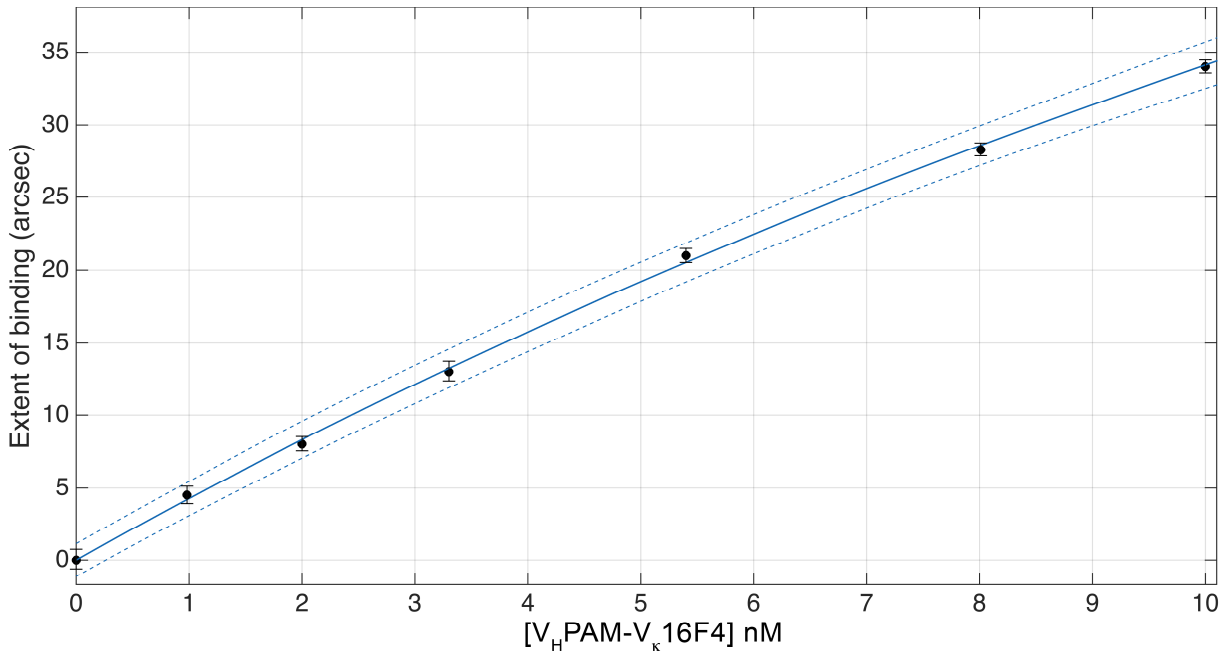

Fig.3. SSc autoantibodies calibration curve. Fit to equation 3 (solid line) and 95% confidence bound (dashed lines) are reported. Each experimental point was the average of three replicates (standard errors of the mean are shown). V_HPAM-V_κ16F4 was used as external calibrator.

To calculate SSc IgG concentrations from ELISA assay and properly compare the results with biosensor data, V_HPAM-V_κ16F4 was used also to generate an analogous hyperbolic calibration curve for ELISA raw data,

$$Abs_{eq} = \frac{Abs_{max}[V_H PAM\text{-}V_k 16F4]}{K_{D,ELISA} + [V_H PAM\text{-}V_k 16F4]} \qquad \text{(Eq.4)}$$

best fitted values for $Abs_{max,E}$ and $K_{D,ELISA}$ being 5.26±1.31 absorbance units and 10.6±3.4 nM.

3.4. Quantification of anti-PDGFRα antibodies in IgG purified from serum

Different dilutions of IgG samples were evaluated to minimize background signal due to cross-reactivity with non-SSc IgGs and decrease the biosensor response within the calibration range. 1:8 dilution of IgG samples in PBS buffer was adopted throughout. Additionally, lower dilution factors were excluded as they were associated to lower discriminating ability among different SSc samples: in fact, the levels of anti-PDGFRα IgG in non-diluted, 1:2 and 1:4 diluted samples were closer to saturating values for rhPDGFRα surface (corresponding to regions of the calibration curve with lower slope). Moreover, the 1:8 dilution was critical in reducing the time requested for surface regeneration (under the adopted dilution, regeneration procedures required less than 15 min).

Limits of detection (LOD) and quantification (LOQ) of the proposed biosensor for anti-PDGFRα IgG (calculated as described in the Materials and Methods Section) were 2.18 and 3.08 nanoequivalents/litre (neq/L) of V_HPAM-V_κ16F4, respectively.

For each IgG sample, three replicates were independently tested, and each sample was analysed in triplicate. Using the V_HPAM-V_κ16F4 calibration curve, it was possible to detect and quantify anti-PDGFRα IgG in all the 8 SSc IgG samples (3.24-4.72 neq/L range) (Table 2A).

A

	SSc									
	SERUM				PURIFIED IgG					
ID	Direct ELISA		Competitive ELISA		Direct ELISA		Competitive ELISA		Biosensor	
	Abs (A.U.)	PDGFRα IgG (nEq/L)	% Abs inhibition	Agonistic PDGFRα IgG	Abs (A.U.)	PDGFRα IgG (nEq/L)	% Abs inhibition	Agonistic PDGFRα IgG	Response (arcsec)	PDGFRα IgG (nEq/L)
SSc1	0.583 ± 0.117	1.34 ± 0.35	55.1 ± 6.1	Pos	0.211 ± 0.059	< LOQ*	42.0 ± 5.9	Pos	16.1 ± 0.7	4.10 ± 0.18
SSc2	0.456 ± 0.205	1.15 ± 0.20	49.8 ± 5.5	Pos	1.635 ± 0.360	4.80 ± 0.18	44.9 ± 3.6	Pos	14.0 ± 0.5	3.58 ± 0.14
SSc3	0.335 ± 0.121	0.66 ± 0.17	45.0 ± 6.3	Pos	0.209 ± 0.056	< LOQ*	43.1 ± 5.2	Pos	16.0 ± 0.7	4.09 ± 0.19
SSc4	0.180 ± 0.081	< LOQ*	44.7 ± 3.6	Pos	0.143 ± 0.030	< LOQ*	27.2 ± 2.7	Neg	13.1 ± 0.4	3.27 ± 0.11
SSc5	0.269 ± 0.051	0.55 ± 0.17	35.3 ± 3.9	Pos	0.928 ± 0.251	2.20 ± 0.14	42.8 ± 4.3	Pos	14.1 ± 0.6	3.59 ± 0.14
SSc6	0.259 ± 0.047	< LOQ*	34.1 ± 3.1	Pos	0.424 ± 0.127	0.88 ± 0.12	51.6 ± 4.6	Pos	18.2 ± 0.6	4.72 ± 0.17
SSc7	0.281 ± 0.081	0.62 ± 0.35	29.9 ± 3.0	Pos	0.130 ± 0.040	< LOQ*	0.40 ± 0.32	Neg	12.9 ± 0.6	3.24 ± 0.14
SSc8	0.111 ± 0.051	< LOQ*	24.1 ± 3.9	Neg	0.189 ± 0.057	< LOQ*	51.0 ± 6.6	Pos	17.1 ± 0.8	4.39 ± 0.21

B

	HC									
	SERUM				PURIFIED IgG					
ID	Direct ELISA		Competitive ELISA		Direct ELISA		Competitive ELISA		Biosensor	
	Abs (A.U.)	PDGFRα IgG (nEq/L)	% Abs inhibition	Agonistic PDGFRα IgG	Abs (A.U.)	PDGFRα IgG (nEq/L)	% Abs inhibition	Agonistic PDGFRα IgG	Response (arcsec)	PDGFRα IgG (nEq/L)
HC1	0.266 ± 0.122	0.53 ± 0.21	37.3 ± 5.6	Pos	0.042 ± 0.010	< LOD*	12.4 ± 1.1	Neg	8.1 ± 0.5	< LOD**
HC2	0.174 ± 0.064	< LOQ*	33.3 ± 2.7	Pos	0.057 ± 0.015	< LOD*	-	Neg	7.4 ± 0.6	< LOD**
HC3	0.164 ± 0.071	< LOQ*	29.8 ± 4.8	Pos	0.139 ± 0.039	< LOQ*	-	Neg	12.0 ± 0.4	< LOQ**
HC4	0.118 ± 0.054	< LOQ*	28.6 ± 3.4	Neg	0.019 ± 0.010	< LOD*	3.4 ± 0.5	Neg	7.0 ± 0.7	< LOD**
HC5	0.190 ± 0.042	< LOQ*	27.8 ± 3.1	Neg	0.051 ± 0.012	< LOD*	12.3 ± 1.4	Neg	7.2 ± 0.6	< LOD**
HC6	0.300 ± 0.084	0.64 ± 0.15	26.7 ± 3.2	Neg	0.012 ± 0.008	< LOD*	-	Neg	6.0 ± 0.4	< LOD**
HC7	0.922 ± 0.313	1.79 ± 0.26	26.3 ± 3.4	Neg	0.066 ± 0.012	< LOD*	19.7 ± 2.0	Neg	7.0 ± 0.8	< LOD**
HC8	0.164 ± 0.036	< LOQ*	21.2 ± 1.7	Neg	0.124 ± 0.026	< LOQ*	-	Neg	7.8 ± 0.5	< LOD**

Table 2. Comparison of results obtained with direct and competitive ELISA tests on both serum and IgG extracts, and with the rhPDGFRα-functionalized biosensor on IgG extracts. Raw as well as corresponding qualitative/quantitative data for SSc (A) and HC samples (B) are provided. Data are presented as mean value of three measurements and standard error of the mean. *LOD and LOQ calculated for direct ELISA assay; **LOD and LOQ calculated for biosensor method.

SSc7 was the only sample being on the edge of significant difference from LOQ, whereas all IgG samples from other patients were significantly higher than LOQ.

Conversely, only 1 out of 8 HC IgG was positive for anti-PDGFRα IgG, but under the quantification threshold of the biosensor (Table 2B).

Due to the small number of samples, all intentionally selected among patients with a more severe disease phenotype, any statistical comparison was of limited utility. Nevertheless, two major sub-groups with statistically different SSc IgG content were identified (Group 1: SSc2, SSc4, SSc5 and SSc7; Group 2: SSc1, SSc3, SSc6 and SSc8). Concerning intra-group comparison, non-significant differences were observed in SSc IgG content among patients SSc1, SSc3, and SSc8. Additionally, SSc8 was not statistically different from SSc6. No significant difference was observed among SSc2, SSc4, SSc5 and SSc7.

3.5. Correlation between biosensor and ELISA data

The same IgG preparations were also tested by ELISA, both in the direct and in the competitive formats previously reported [9].

Comparative analysis revealed the lower sensibility of the direct ELISA: in fact, using the V_HPAM-V_κ16F4 calibration curve, anti-PDGFRα IgG were quantified by the biosensor assay in all SSc samples, whereas only 5 out of 8 SSc serum samples, and 3 out of 8 SSc IgG samples were quantified by direct ELISA (LOD and LOQ of the direct ELISA assay values were 0.21 and 0.50 nEq/L) (Table 2A). The competitive ELISA, potentially representing the most specific method to

detect agonistic anti-PDGFRα IgG in both serum and purified IgG samples, was shown to be a merely qualitative method, because the threshold inhibition values for the presence/absence and for the quantification of agonistic anti-PDGFRα IgG were 29.7% and 79.0%, respectively, indicating that only for absorbance reductions higher than 79% it would be possible to correctly determine anti-PDGFRα IgG concentration, Unfortunately, such inhibition percentage is way higher than what we observed in all analyzed samples.

On the other hand, all the 8 HC IgG samples were double negative, except for HC 3 and 8 that tested positive by direct but not by competitive ELISA (Table 2B); interestingly, HC3 tested positive also by biosensor assay.

3.6. Reusability and efficiency of the biosensor

Different regeneration conditions were tested. The complete dissociation of the recombinant human mAb/rhPDGFRα complexes was performed by washes with both mild acidic (HCl 10 mM) and with buffer solutions (the PBS binding buffer, with pH set to 5.5). Using 10 mM HCl, the biosensor surface could be used without any loss of activity for at least 10 measurement cycles before significant loss of binding capacity was reported. Conversely, the sensing surface resisted to a higher number of experimental cycles (biosensor response did not change by more than 5% after 50 regeneration cycles) when PBS pH=5.5 was used (K_D for the antigen-antibody complex was approximately 50-fold higher at pH 5.5). Subsequently, the use of this buffer solution provided an efficient (even if slower) desorption of the ligand without degrading the immobilized receptor: in fact, although less aggressive than complex dissociation under acidic conditions or using chaotropic agents (both procedures being harmful to the preservation of binding ability, and likely to diminish lifetime of the immobilized molecules), this procedure required longer regeneration times. The reproducibility of the binding assay was dissected by comparison of the intra- and inter-day variability. In line with the results of surface stability evaluation, a single surface (re-used on

different days) could withstand a total number of approximately 50 binding events before experiencing a significant loss of signal (> 5%).

Concerning the inter-day variation of the same surface, the maximal coefficients of variation (5.1% at 10 nM V_HPAM-V_κ16F4, and 4.1% at 1 nM V_HPAM-V_κ16F4, respectively) were within the confidence limits of the calibration curve.

Additionally, the "surface-to-surface" variation of assay sensitivity was assessed by comparing the measured binding affinity of different PDGFRα surface for V_HPAM-V_κ16F4. This variation was negligible, with K_D values ranging within the experimental error, independently of the batches of V_HPAM-V_κ16F4 (the calibrator) and of rhPDGFRα used.

4. Discussion

One of the major advantages of biosensors lies in their versatility, as they can be customized and efficiently used in a wide range of applications [17-20]. Specifically, biosensors (both re-usable and single-use) are gaining an increasing impact on clinical chemistry and diagnosis [21-26].

Under optimized experimental conditions [10], here we characterized the binding kinetics of a unique panel of recombinant human monoclonal autoantibodies with different PDGFRα epitope specificity and biological activity [9, 11]. Tested autoantibodies showed strong specificity (PDGFRβ was not recognized) as well as moderate-to-high affinity for PDGFRα. Interestingly, we observed an affinity range progressively increasing from the non-agonistic antibody V_HPAM-V_κ13B8 to the native ligand PDGF-BB, and we found that V_HPAM-V_κ16F4 agonistic antibody, binding specifically to a conformational motif of the human PDGFRα largely overlapping with the PDGF-BB binding site [9], possessed the binding profile most similar to PDGF-BB. Based on these results, V_HPAM-V_κ16F4 mAb was used to calibrate the biosensor for the selective detection and quantification of human PDGFRα-specific, high affinity, bona fide agonistic, serum IgG autoantibodies, like those expected to be enriched in patients affected by SSc [3]. For biosensor analysis, we employed IgG purified from serum, since whole serum generated an extremely high,

and non-interpretable response upon addition onto rhPDGFRα surface due to multiple non-specific protein-protein interactions, which eclipsed the signal produced by specific rhPDGFRα-SSc IgG recognition. The data obtained herein by applying our novel biosensor assay to 8 SSc and 8 HC IgG samples confirmed the presence of IgG with the aforementioned characteristics in all the SSc samples. This finding was corroborated by comparing the biosensor results with the data obtained by two ELISA methods [9]. In fact, the competitive ELISA, which detects only anti-PDGFRα antibodies sharing the same epitope of the calibrator antibody, confirmed in 6 out of 8 SSc IgG samples the positivity obtained by biosensor. Only in two SSc IgG samples (SSc 4 and 7), both positive by biosensor assay, the competitive ELISA was negative but the direct ELISA, which detects all anti-PDGFRα antibodies regardless of their agonistic activity and affinity towards the receptor, was positive, indicating the presence of anti-PDGFRα antibodies directed to an epitope different from that recognized by the calibrator antibody. This suggests that the biosensor is not completely specific for anti-PDGFRα antibodies sharing the same epitope of the calibrator antibody, still it is specific for high affinity anti-PDGFRα antibodies. On the other hand, we intentionally selected for this study 8 HC IgG samples with previous ambiguous serological results (Table 2B), in order to test the ability of our new method to identify such samples as negative, which was indeed the case in 7 out of 8 samples. Of these negative HC IgG samples, 6 were confirmed by direct ELISA. The only HC IgG testing positive by biosensor (HC3), was however under the biosensor quantification threshold. It was positive also by direct ELISA, but negative by competitive ELISA. This signal may be due to traces of high-affinity, non-agonistic anti-PDGFRα antibodies like V_HPAM-V_κ13B8. Taken altogether, the comparison between the new biosensor assay and the previously described ELISAs indicates a remarkable concordance, although in a small sample number. Thus, this must be replicated in a larger cohort in future studies. Despite this limitation, the inter-assay comparison indicates that the most relevant features of the biosensor assay are the selective detection and the quantification of high affinity anti-PDGFRα antibodies. These characteristics make this assay a valuable complementary tool to the direct ELISA, or even

an alternative tool when screening samples for agonistic anti-PDGFRα autoantibodies only. For the latter aim, the biosensor seems to be better suited than the competitive ELISA previously described, not only for the higher sensitivity but also for the shorter assay time, the lower consumption of reagents, and the lower cost per single analysis (Table 3). In fact, the competitive ELISA is characterized by an additional step consisting in the sample pre-incubation with a soluble peptide, with subsequent problems in terms of assay standardization and rapidity. Nonetheless, the real-time monitoring of biosensor response allows to check proper folding/orientation of rhPDGFRα upon immobilization.

	Direct ELISA	Competitive ELISA	Proposed Biosensor
Time for surface preparation	24 h*	24 h*	50 min
Time *per* analysis	24 h*	48 h**	6-15 min
Number of analyses *per* well	1	1	50
Maximum number of simultaneous analyses	96	96	1
Cost *per* plate/cuvette	384 €	768 €	250 €
Cost *per* single analysis	4 €	8 €	5 €
Type of detection	Indirect: end-point absorbance reading	Indirect: end-point absorbance reading	Direct: label-free and real-time monitoring

Table 3. Comparison of costs and time associated with (direct and competitive) ELISA and the proposed biosensor assay (*overnight incubation required; ** two-overnight incubation required).

Moreover, the interpretation of the ELISA data requires a not trivial analytical step consisting in the determination of the optimal cut-off value by ROC curve. Conversely, the biosensor provides unambiguous responses upon the binding of high affinity anti-PDGFRα antibodies within one minute. Thus, it is possible to perform a quick screening of multiple samples (collectively requiring about one hour for the purification of IgG from serum).

Besides these aspects, the biosensor assay holds another major advantage towards the ELISA, that is the quantification ability. This feature is relevant for an assay designed to measure the levels of

autoantibodies in human samples as biomarkers of SSc disease. In point of fact, we intentionally selected for this study 8 serum/IgG samples taken from patients with a more severe disease phenotype, in order to test the ability of our method to detect and measure anti-PDGFRα antibody levels in those patients who in real life would benefit from a quantifiable biomarker, e.g. during therapy. Of course, it will be mandatory applying this novel biosensor assay to samples taken from patients at different stages of disease to assess if high affinity anti-PDGFRα antibodies are sensitive to disease change and are, therefore, suitable as SSc biomarkers. This would fill an important gap in the current management of different SSc patients' subsets [27].

ACKNOWLEDGMENTS

This work was supported by Gruppo Italiano Lotta alla Sclerodermia (GILS Young Investigator Award to Dr. Moroncini), Associazione Italiana Lotta alla Sclerodermia (AILS) and grant RF-2011-02352331 from Ministero Italiano della Salute (to Dr. Gabrielli).

REFERENCES

[1] A. Gabrielli, E.V. Avvedimento, T. Krieg, Scleroderma, N Engl J Med, 360 (2009) 1989-2003.
[2] C. Mohan, S. Assassi, Biomarkers in rheumatic diseases: how can they facilitate diagnosis and assessment of disease activity?, BMJ, 351 (2015) h5079.
[3] S.S. Baroni, M. Santillo, F. Bevilacqua, M. Luchetti, T. Spadoni, M. Mancini, P. Fraticelli, P. Sambo, A. Funaro, A. Kazlauskas, E.V. Avvedimento, A. Gabrielli, Stimulatory autoantibodies to the PDGF receptor in systemic sclerosis, N Engl J Med, 354 (2006) 2667-2676.
[4] S. Smaldone, J. Olivieri, G.L. Gusella, G. Moroncini, A. Gabrielli, F. Ramirez, Ha-Ras stabilization mediates pro-fibrotic signals in dermal fibroblasts, Fibrogenesis Tissue Repair, 4 (2011) 8.
[5] M.M. Luchetti, G. Moroncini, M.J. Escamez, S.S. Baroni, T. Spadoni, A. Grieco, C. Paolini, A. Funaro, E.V. Avvedimento, F. Larcher, M. Del Rio, A. Gabrielli, Induction of scleroderma fibrosis in skin-humanized mice by anti-Platelet-Derived Growth Factor receptor agonistic autoantibodies, Arthritis Rheumatol, (2016).
[6] J.F. Classen, D. Henrohn, F. Rorsman, J. Lennartsson, B.R. Lauwerys, G. Wikstrom, C. Rorsman, S. Lenglez, K. Franck-Larsson, J.P. Tomasi, O. Kampe, M. Vanthuyne, F.A. Houssiau, J.B. Demoulin, Lack of evidence of stimulatory autoantibodies to platelet-derived growth factor receptor in patients with systemic sclerosis, Arthritis Rheum, 60 (2009) 1137-1144.

[7] N. Loizos, L. Lariccia, J. Weiner, H. Griffith, F. Boin, L. Hummers, F. Wigley, P. Kussie, Lack of detection of agonist activity by antibodies to platelet-derived growth factor receptor alpha in a subset of normal and systemic sclerosis patient sera, Arthritis Rheum, 60 (2009) 1145-1151.
[8] A. Gabrielli, G. Moroncini, S. Svegliati, E.V. Avvedimento, Autoantibodies against the platelet-derived growth factor receptor in scleroderma: comment on the articles by Classen et al and Loizos et al, Arthritis Rheum, 60 (2009) 3521-3522.
[9] G. Moroncini, A. Grieco, G. Nacci, C. Paolini, C. Tonnini, K.N. Pozniak, M. Cuccioloni, M. Mozzicafreddo, S. Svegliati, M. Angeletti, A. Kazlauskas, E.V. Avvedimento, A. Funaro, A. Gabrielli, Epitope specificity determines pathogenicity and detectability of anti-PDGFRalpha autoantibodies in systemic sclerosis, Arthritis Rheumatol, (2015).
[10] M. Cuccioloni, Biosensor-based Binding Assay for Platelet-Derived Growth Factor Receptor-α Autoantibodies in Human Serum, Journal of Analytical & Bioanalytical Techniques, S7 (2013).
[11] G. Nacci, G. Moroncini, A. Grieco, C. Paolini, M. Cuccioloni, M. Mozzicafreddo, K. Pozniak, C. Tonnini, S. Svegliati, M. Angeletti, E. Avvedimento, A. Funaro, A. Gabrielli, Isolation and cloning of stimulatory anti-PDGF receptor auto-antibodies from the immunological repertoire of patients with systemic sclerosis, Febs J, 278 (2011) 253-253.
[12] R. Cush, J.M. Cronin, W.J. Stewart, C.H. Maule, J. Molloy, The resonant mirror: a novel optical biosensor for direct sensing of biomolecular interactions Part I: Principle of operation and associated instrumentation, Biosens Bioelectron, 8 (1993) 347-354.
[13] T.E. Plowman, J.D. Durstchi, H.K. Wang, D.A. Christensen, J.N. Herron, W.M. Reichert, Multiple-analyte fluoroimmunoassay using an integrated optical waveguide sensor, Anal Chem, 71 (1999) 4344-4352.
[14] R.J. Davies, P.R. Edwards, H.J. Watts, C.R. Lowe, P.E. Buckle, The resonant mirror: a versatile tool for the study of biomolecular interactions, 1994.
[15] E.C. LeRoy, C. Black, R. Fleischmajer, S. Jablonska, T. Krieg, T.A. Medsger, Jr., N. Rowell, F. Wollheim, Scleroderma (systemic sclerosis): classification, subsets and pathogenesis, J Rheumatol, 15 (1988) 202-205.
[16] J. Inczedy, T. Lengyel, A.M. Ure, Compendium of Analytical Nomenclature - The Orange Book., in: B. Science (Ed.)1998.
[17] M. Cuccioloni, L. Sparapani, M. Amici, G. Lupidi, A.M. Eleuteri, M. Angeletti, Kinetic and equilibrium characterization of the interaction between bovine trypsin and I-ovalbumin, Biochim Biophys Acta, 1702 (2004) 199-207.
[18] M. Cuccioloni, M. Mozzicafreddo, M. Spina, C.N. Tran, M. Falconi, A.M. Eleuteri, M. Angeletti, Epigallocatechin-3-gallate potently inhibits the in vitro activity of hydroxy-3-methyl-glutaryl-CoA reductase, J Lipid Res, 52 (2011) 897-907.
[19] M. Cuccioloni, M. Mozzicafreddo, S. Barocci, F. Ciuti, I. Pecorelli, A.M. Eleuteri, M. Spina, E. Fioretti, M. Angeletti, Biosensor-based screening method for the detection of aflatoxins B1-G1, Anal Chem, 80 (2008) 9250-9256.
[20] M. Cuccioloni, M. Amici, A.M. Eleuteri, M. Biagetti, S. Barocci, M. Angeletti, Binding of recombinant PrPc to human plasminogen: kinetic and thermodynamic study using a resonant mirror biosensor, Proteins, 58 (2005) 728-734.
[21] T.R. Holford, F. Davis, S.P. Higson, Recent trends in antibody based sensors, Biosens Bioelectron, 34 (2012) 12-24.
[22] J.R. Conway, N.O. Carragher, P. Timpson, Developments in preclinical cancer imaging: innovating the discovery of therapeutics, Nat Rev Cancer, 14 (2014) 314-328.
[23] A. Buhl, J.H. Metzger, N.H. Heegaard, P. von Landenberg, M. Fleck, P.B. Luppa, Novel biosensor-based analytic device for the detection of anti-double-stranded DNA antibodies, Clin Chem, 53 (2007) 334-341.
[24] C.I. Justino, A.C. Duarte, T.A. Rocha-Santos, Immunosensors in Clinical Laboratory Diagnostics, Adv Clin Chem, 73 (2016) 65-108.

[25] N.S. Fracchiolla, S. Artuso, A. Cortelezzi, Biosensors in clinical practice: focus on oncohematology, Sensors (Basel), 13 (2013) 6423-6447.
[26] N.Y. Kim, K.K. Adhikari, R. Dhakal, Z. Chuluunbaatar, C. Wang, E.S. Kim, Rapid, sensitive, and reusable detection of glucose by a robust radiofrequency integrated passive device biosensor chip, Sci Rep, 5 (2015) 7807.
[27] S.R. Johnson, M. Hinchcliff, Y. Asano, Controversies: molecular vs. clinical systemic sclerosis classification, J scleroderma relat disord, 1 (2016) 277 - 285.

GRAPHICAL ABSTRACT

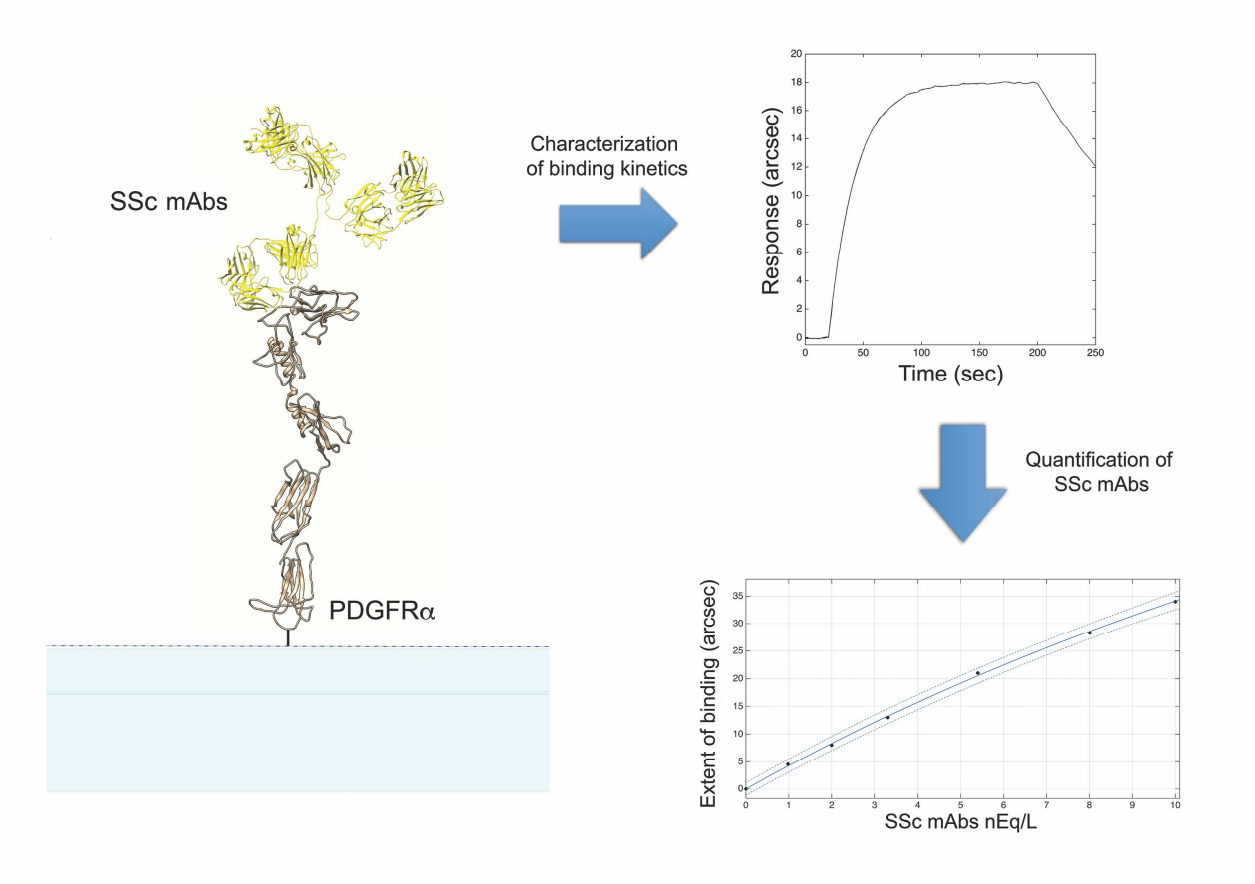

HIGHLIGHTS

A platelet-derived growth factor receptor α-based biosensor is presented.

High-affinity specific interactions are observed between surface-blocked receptor and autoantibodies.

The biosensor can detect and quantify high-affinity anti-PDGFRα autoantibodies in total serum IgG, thus discriminating SSc patients from healthy controls.